NeuroImage: Clinical 27 (2020) 102285

Contents lists available at ScienceDirect

NeuroImage: Clinical

journal homepage: www.elsevier.com/locate/ynicl

Mapping typical and hypokinetic dysarthric speech production network using a connected speech paradigm in functional MRI

Shalini Narayana[a,b,c,*,1], Megan B. Parsons[d,1], Wei Zhang[e], Crystal Franklin[e], Katherine Schiller[a], Asim F. Choudhri[b,f], Peter T. Fox[e], Mark S. LeDoux[g,h], Michael Cannito[i]

[a] Department of Pediatrics, Division of Pediatric Neurology, University of Tennessee Health Science Center, Memphis, TN 38103, USA
[b] Neuroscience Institute, Le Bonheur Children's Hospital, Memphis, TN 38103, USA
[c] Department of Anatomy and Neurobiology, University of Tennessee Health Science Center, Memphis, TN 38103, USA
[d] School of Communication Sciences and Disorders, University of Memphis, Memphis, TN 38152, USA
[e] Research Imaging Institute, University of Texas Health San Antonio, San Antonio, TX 78229, USA
[f] Department of Radiology, Division of Neuroradiology, University of Tennessee Health Science Center, Memphis, TN 38103, USA
[g] Veracity Neuroscience LLC, Memphis, TN 38157, USA
[h] Department of Psychology and School of Health Studies, University of Memphis, Memphis, TN 38152, USA
[i] Department of Communicative Disorders, University of Louisiana at Lafayette, USA

ARTICLE INFO

Keywords:
Speech production
Speech production network
Connected speech
Hypokinetic dysarthria
Normal speech
PET
fMRI
Motor speech disorders

ABSTRACT

We developed a task paradigm whereby subjects spoke aloud while minimizing head motion during functional MRI (fMRI) in order to better understand the neural circuitry involved in motor speech disorders due to dysfunction of the central nervous system. To validate our overt continuous speech paradigm, we mapped the speech production network (SPN) in typical speakers (n = 19, 10 females) and speakers with hypokinetic dysarthria as a manifestation of Parkinson disease (HKD; n = 21, 8 females) in fMRI. We then compared it with the SPN derived during overt speech production by ^{15}O-water PET in the same group of typical speakers and another HKD cohort (n = 10, 2 females). The fMRI overt connected speech paradigm did not result in excessive motion artifacts and successfully identified the same brain areas demonstrated in the PET studies in the two cohorts. The SPN derived in fMRI demonstrated significant spatial overlap with the corresponding PET derived maps (typical speakers: r = 0.52; speakers with HKD: r = 0.43) and identified the components of the neural circuit of speech production belonging to the feedforward and feedback subsystems. The fMRI study in speakers with HKD identified significantly decreased activity in critical feedforward (bilateral dorsal premotor and motor cortices) and feedback (auditory and somatosensory areas) subsystems replicating previous PET study findings in this cohort. These results demonstrate that the overt connected speech paradigm is feasible during fMRI and can accurately localize the neural substrates of typical and disordered speech production. Our fMRI paradigm should prove useful for study of motor speech and voice disorders, including stuttering, apraxia of speech, dysarthria, and spasmodic dysphonia.

1. Introduction

Although the organization of neural structures involved in speech production is becoming increasingly well-understood from existing positron emission tomography (PET) and functional magnetic resonance imaging (fMRI) data (Price, 2010, 2012), relatively few studies have explored the use of continuous speech tasks in block design fMRI (Brown et al., 2009; Abo et al., 2009). Most of our understanding about

Abbreviations: PET, Positron Emission Tomography; fMRI, functional Magnetic Resonance Imaging; SPN, Speech Production Network; HKD, hypokinetic Dysarthria; rCBF, regional Cerebral Blood Flow; MEG, Magnetoencephalography; SMA, Supplemental Motor Area; PD, Parkinson Disease; ASL, Arterial Spinal Labeling; BOLD, Blood Oxygenation Level Dependent; FWHM, Full Width at Half Maximum; TR, Repetition Time; TE, Echo Time; MCFLIRT, Motion Correction and Linear Image Registration Tool; FSL, FMRIB Software Library; MNI, Montreal Neurological Institute; DICOM, Digital Imaging and Communications in Medicine; GUI, Graphical User Interface; MIPS, Multiple Image Processing Station; SPI{z}), Statistical Parametric Image of z score; FEAT, FMRI Expert Analysis Tool; FLAME, FMRIB's Local Analysis of Mixed Effects; PMd, dorsal PreMotor cortex; BA, Brodmann Area; DIVA, Directions into Velocities of Articulators; M1, Primary Motor Cortex

* Corresponding author at: Department of Pediatrics, Division of Pediatric Neurology, University of Tennessee Health Science Center, Memphis, TN 38103, USA.
E-mail address: snaraya2@uthsc.edu (S. Narayana).

[1] Shalini Narayana and Megan B. Parsons contributed equally to this manuscript.

https://doi.org/10.1016/j.nicl.2020.102285
Received 25 January 2020; Received in revised form 13 May 2020; Accepted 17 May 2020
Available online 01 June 2020
2213-1582/ © 2020 The Author(s). Published by Elsevier Inc. This is an open access article under the CC BY-NC-ND license (http://creativecommons.org/licenses/BY-NC-ND/4.0/).

neural circuits engaged during connected speech production comes from PET studies as PET is less affected by the movement of the jaw, lips and head that are associated with overt connected speech (Price, 2010). However, few centers have access to PET and radiation risks make it less accessible to children and less repeatable in adults. In contrast, fMRI is readily available for all age groups and has no limits on the number of scanning sessions. A major limitation of fMRI has been overt speech-induced motion artifacts. Therefore, researchers continue to use covert reading tasks in an effort to minimize motion artifact while measuring cortical activation related to speech production (Hesling et al., 2019; Tourville et al., 2019).

The use of covert speech tasks is advantageous if one were to assume that covert speech involves all of the processes and neural mechanisms of overt speech except for motor production. However, this assumption that covert speech plus motor production equals overt speech has not been clearly established in the literature. There has been some research that indicated similar patterns of activation when comparing covert to overt speech with the exception of the motor activation observed in overt speech (Palmer et al., 2001). On the other hand, several studies using fMRI (Barch et al., 1999; Huang et al., 2002; Shuster and Lemieux, 2005), MEG (Numminen and Curio, 1999), and regional cerebral blood flow (rCBF) measures (Ryding et al., 1996) have failed to validate this assumption in typical speakers or in patients with speech disorders (Arnold et al., 2014). There is evidence that tasks performed overtly engage not only the primary motor cortex but also the supplemental motor area (SMA) and dorsal premotor cortex (Partovi et al., 2012; Palmer et al., 2001; Kielar et al., 2011). Importantly, covert speech tasks do not engage auditory and somatosensory feedback regions including bilateral superior temporal gyri, right ventral premotor cortex, and parietal cortex which monitor speech output on aspects such as content, grammaticality, fluency and volume (Shuster and Lemieux, 2005; Tourville et al., 2008) and position of articulators and tongue (Guenther, 2016). This feedback loop is very important in speech production as it assures correct and proper speech output (Levelt et al., 1999). Hence while covert speech tasks are relatively well-suited to examine the feedforward subsystem of the speech production network (SPN), it is not amenable to studying the feedback subsystem.

Researchers have previously used single words tasks and short phrases to investigate both the feedforward and feedback subsystems of SPN engaged during speaking aloud in fMRI (Guenther, 2016; Tourville et al., 2008). However, since sparse sampling techniques are used, the signal-to-noise ratio is inefficient and requires a large number of stimuli, which extends the length of the study. Further, these tasks are not suited to study motor speech disorders (e.g. stuttering, dysarthria, and apraxia) where disordered speech patterns resulting from deficits in fluency, articulation, and volume are most evident during connected speech. For example, voice and speech abnormalities in individuals with hypokinetic dysarthria secondary to Parkinson disease (PD) are most evident during overt speech tasks. Therefore, connected speech tasks may be the most effective when examining SPN in its entirety (i.e., both feedforward and feedback subsystems).

Previous research has indicated that arterial spinal labeling (ASL) can be used during overt speech production tasks (Kemeny et al., 2005) and narration tasks (Troiani et al., 2008). These studies, however, have a few drawbacks. First, ASL is harder to utilize when compared to blood oxygenation level dependent fMRI (BOLD-fMRI), has a lower signal-to-noise ratio, and is not as robust as the BOLD signal, making it a less than ideal method to use. Next, spontaneous sentence and narration production tasks lead to variance in individual performance since they fully engage the processes of sematic and linguistic formulation. Further, narrative production may be harder to replicate when tested multiple times. An oral paragraph reading task, on the other hand, is a more robust, reliable production task that can be used across various populations and for pre- and post- intervention assessments.

Until now, relatively few studies have explored the use of continuous speech tasks in block design fMRI (Brown et al., 2009; Abo et al., 2009). In comparison to event-related paradigms, block design fMRI is simpler to acquire and process, and it can offer a higher signal-to-noise ratio, due to a comparatively large number of data points (Amaro and Barker, 2006). Reading standardized passages is also easier for participants to learn and perform as compared to spontaneous speech tasks. Having a printed text to read imposes much less linguistic burden on a literate speaker and allows for linguistic features to remain stable across repeated imaging sessions for longitudinal research.

One concern with using connected speech tasks is the presence of motion artifact. The movement of the structures related to speech during volume acquisition has been shown to be the most significant source of head motion artifact (Birn et al., 1998,1999; Huang et al., 2002). However, by using modified reading with a closed jaw and minimal lip movement, researchers can significantly limit movement artifact noted during normal speech. Although producing speech without moving the jaw and lips may adversely affect clarity, due to articulatory compensation, the speech is still voiced. The laryngeal motor cortex has been successfully identified using phrases that were vocalized without moving any articulators (Murphy et al., 1997) as well as using a task similar to that being evaluated here (Brown et al., 2009). Furthermore, In typical speakers, restricting jaw movement during speech (for instance using small bite blocks) did not significantly affect speech quality despite diminishing its clarity and naturalness (Baum et al., 1996; Lane et al., 2005; Solomon et al., 2016), indicating that processing of the audio signal as well as the auditory feedback mechanisms during speaking without moving jaws and lips are not substantially affected. Therefore, the brain regions activated during phonation and regions mediating auditory and somatosensory feedback can be identified by this modified speech paradigm. Further, motion correction algorithms have improved over the past few decades, and the location of the motion artifacts that may result from small jaw movements does not impede the identification of language/speech areas (Tamura et al., 2002).

Obviously, speaking with the jaw closed is atypical speech production; however, it does occur at times in naturalistic communication as with speaking with teeth clenched, with a pipe stem held between the teeth, or with the jaw wired shut post-surgery. Such speech remains reasonably understandable and is similar to speaking with a bite block positioned between the teeth to restrict jaw movement. Bite-block speech in typical speakers has been well studied. It has been demonstrated to adapt immediately for various acoustic speech characteristics including vowel formant frequencies (Kelso and Tuller, 1983; Gay et al., 1981; Lindblom et al., 1977; McFarland et al., 1996), vowel and consonant durations (Smith, 1987), and coarticulation (Sussman et al., 1995). Moreover, jaw-closed speech has been shown to have consonant and vowel durations more similar to unconstrained speech than does bite-block speech. While studies of bite-block speech in PD are limited, it has been shown to adapt immediately for vowel formant frequencies (Gabbert, 2005; Mefferd and Bissmeyer, 2016). Therefore, we hypothesize that speaking with jaw closed and limited lip movement should sufficiently approximate unconstrained speech to appropriately activate the SPN for both typical speakers and those with PD.

As previously mentioned, it would be of interest to map SPN in patients with speech and voice disorders. For example, research has indicated that up to 90% of patients diagnosed with PD are affected by motor speech deficits collectively termed hypokinetic dysarthria (HKD) (Duffy, 2005; Ho et al., 1999). Research on whether the SPN differs between speakers with HKD and typical speakers has been limited to few studies that have used either overt speech paradigms in PET (Narayana et al., 2010; Pinto et al., 2004) or overt reading of single words or sentences in fMRI (Arnold et al., 2014; Rektorova et al., 2007; Saxena et al., 2014; Maillet et al., 2012; Pinto et al., 2011).

Thus, the purpose of the present study was to first validate the SPN obtained in typical speakers using overt continuous speech in a block design fMRI paradigm by comparing it to the network identified by PET

in the same individuals. Next, we compared the SPN map obtained in speakers with HKD using continuous speech in a block design fMRI paradigm to the map identified previously by PET (Narayana et al., 2010). In both speaker groups, we hypothesized that the SPN derived from the new fMRI paradigm will closely match that obtained by PET. Finally, the study compared the SPN of speakers with HKD to those of typical speakers derived from overt continuous speech paradigms in PET and fMRI. Here we expected that the changes in the neural circuits of speech production in HKD previously observed (Liotti et al., 2003; Pinto et al., 2004) would be replicated in the PET data and that these changes could also be identified using the new connected speech paradigm in fMRI.

2. Methods

2.1. Participants

2.1.1. Typical speakers

Forty-two right-handed individuals (22 males; mean age 31.6 ± 9.7 years) with no history of neurological or psychiatric illness were enrolled in the study after approval by the institutional review board at the University of Texas Health Science Center at San Antonio. An informed consent was obtained from all participants in accordance with the Declaration of Helsinki, and participants were compensated for their time. In all participants, hearing was screened and the handedness confirmed by Edinburgh inventory (Oldfield, 1971). Two participants failed hearing screen and 3 participants dropped out of the study due to time constraints. Of the thirty seven individuals who proceeded to complete fMRI and other study procedures, 19 completed PET imaging. Data from 19 participants (10 females, mean age 29 ± 9 years) who completed speech motor mapping by both PET and fMRI are reported here.

2.1.2. Speakers with HKD

2.1.2.1. PET study. Ten right-handed participants (8 males, mean age 60 ± 11 years) with a diagnosis of PD and hypokinetic dysarthria were enrolled in the study after approval by University of Texas Health Science Center at San Antonio Institutional Review Board. The participants were part of a study that examined the neural correlates of efficacy of voice therapy and the results have been published previously (Narayana et al., 2010).

2.1.2.2. fMRI study. Thirty-nine individuals with PD (24 males, mean age 70 ± 7 years) and hypokinetic dysarthria were enrolled in the study that examined the changes in the speech motor system following voice therapy after approval by the University of Tennessee Health Science Center at Memphis Institutional Review Board. An informed consent was obtained from all participants in accordance with the Declaration of Helsinki, and participants were compensated for their time. During voice and speech screening, six participants were deemed to have only mild hypophonia and were therefore ineligible to continue in the study. In four patients, the diagnosis of Parkinson Disease was revised during screening neurological examination (multiple system atrophy (n = 1), progressive supranuclear palsy (n = 2) and functional movement disorder (n = 1)) and therefore withdrawn from the study. Four patients withdrew from the study due to scheduling conflicts. One patient was found to have a preexisting tongue and throat condition during laryngology screening and was found to be ineligible to continue in the study. Of the 24 patients who proceeded to complete baseline fMRI, 3 patients did not complete the reading task due poor visual acuity. Twenty-one patients (13 males, 18 right-handed, 2 left-handed, one ambidextrous; mean age 69 ± 9) with moderate to severe HKD who completed a reading task in fMRI are included in the analysis.

In all individuals with PD (in the PET and fMRI studies), the diagnosis was verified by a board-certified neurologist with subspecialty expertise in movement disorders in accordance with UK Parkinson Disease Society Brain Bank Diagnostic Criteria. The speech was initially evaluated by the clinician completing the UPDRS (item 18) and a certified speech language pathologist (SLP) determined the severity of hypophonia, as well as characterized other aspects of the participants' hypokinetic dysarthria in terms of pitch, voice quality, articulation, rate, resonance, respiration, and prosody (Darley et al., 1975). Participants were screened for any history of hearing impairment or other neurologic or psychiatric diseases and underwent a laryngeal examination to rule out abnormalities that might affect the participation in voice therapy and treatment outcomes (e.g., gastric reflux and vocal fold paralysis). All individuals were on some form of dopaminergic therapy (levodopa, dopamine agonist, and/or monoamine oxidase type B inhibitor). Imaging was carried out during "on" periods. The participants' hearing was screened, and handedness confirmed by Edinburgh inventory (Oldfield, 1971).

2.2. Positron emission tomography

2.2.1. Typical Speakers and Speakers with HKD

PET data were collected from typical speakers (n = 19) and speakers with HKD (n = 10) with a CTI EXACT HR scanner (Knoxville, TN; UT Health San Antonio). Sixty-three contiguous slices (2.5-mm thick) in a transaxial field of view of 15.5 cm were acquired. Water labeled with oxygen-15 ($H_2{}^{15}O$, half-life 122 s) was administered intravenously (555 MBq $H_2{}^{15}O$/scan), and cerebral blood flow (CBF) was measured using a bolus technique (Fox et al., 2006; Fox et al., 2000). Data was collected after bolus arrival in the brain (15–20 s after injection) for 90 s. Images were corrected by measured attenuation using $^{68}Ge/^{68}Ga$ transmission scans and reconstructed at an in-plane resolution of 7-mm full width at half maximum (FWHM) and an axial resolution of 6.5-mm FWHM. Participants' heads were immobilized in the PET scanner using individually fitted, thermally molded, plastic face masks (Fox and Raichle, 1984). During the PET session, participants underwent two measurements of CBF during paragraph reading and during eyes open rest. For the paragraph reading condition, the participants read aloud sections of the Grandfather (Van Riper, 1963; Darley et al., 1975) and the first paragraph of the Rainbow (Fairbanks, 1960) passages. The paragraphs were rehearsed prior to scanning to the extent that they were over-learned as the primary aim of this study was to examine the neural correlates of phonetic encoding, phonology, and articulation and, therefore, reduce activations resulting from semantic and syntactic processing observed during reading novel passages. Additionally, since the face mask covered the chin and restricted the jaw movement, the speakers also practiced reading the passages after the mask was set. Both typical speakers and speakers with HKD were able to read aloud successfully without moving their jaws. During each paragraph reading condition, both passages were displayed over 90 s on a computer monitor screen placed in front of patients' eyes. In the eyes open rest condition, patients were asked to lie still while looking at a crosshair on the monitor and maintain a relaxed state. Along with minimizing head movement during imaging, the individually fitted face mask also limited the movement of jaws and lips during reading. This made the PET reading paradigm similar to that performed in fMRI.

2.3. Functional MRI

A T2*-weighted gradient-echo echo-planar-imaging BOLD-fMRI was acquired as the participants read aloud sections of the Grandfather and the first paragraph of the Rainbow passages in 30 s epochs, alternating with 30 s rest epochs over the course of a 6-min scan. The participants were able to read both passages twice during this time. Similar to the PET study, the passages and reading with closed jaw and lips were rehearsed several times before going into the scanner. The passages were displayed on a computer monitor screen placed behind the scanner and reflected by a mirror placed in front of the participant. Participants read passages with their teeth opposed and without

moving their jaws and lips in order to minimize mouth movement, and by extension, motion artifact. In the eyes open rest condition, participants were asked to lie still while looking at a crosshair on the monitor and maintain a relaxed state.

2.3.1. Typical speakers

A Siemens 3 T-TIM MRI Scanner (Siemens AG, Munich, DE; UT Health San Antonio) with a 12-channel head coil was used to perform structural and functional brain imaging in typical speakers. One hundred and eighty-three (183) volumes with a voxel size of 2 mm × 2 mm × 6 mm, TR of 2000 ms, TE of 30 ms, a flip angle of 90°, and field of view = 128 × 128 × 21 were acquired in an ascending slice order. A high-resolution anatomical image was acquired using a T1 weighted 3-D Turbo- Fast low angle shot sequence (TR/TE/flip angle = 2100/3.04/13°) with an adiabatic inversion contrast pulse (TI = 785 ms), field of view = 220 × 320 × 208, and 0.8 mm^3 spatial resolution.

2.3.2. Speakers with HKD

A Siemens 3 T Verio MRI Scanner (Siemens AG, Munich, DE, UTHSC, Memphis) with a 12-channel head coil was used to perform structural and functional brain imaging in speakers with HKD. One hundred and twenty-three (123) volumes with a voxel size of 2.55 mm × 2.55 mm × 3.5 mm, TR of 3000 ms, TE of 30 ms, a flip angle of 90°, and field of view = 256 × 204 × 40 were acquired in an ascending slice order. After the fMRI, a high-resolution anatomical image was acquired using a T1 weighted 3D sequence (TR/TE/flip angle = 1900/2.93/9°) with slice-select inversion recovery pulse (TI = 900 ms), field of view = 512 × 512 × 176, and 0.5 mm × 0.5 mm × 1 mm spatial resolution.

2.4. Data preprocessing

2.4.1. PET

PET data from the two groups were preprocessed in the same manner using previously validated methods and in-house software. PET images were corrected for head motion using the MCFLIRT tool in FSL 4.0 (http://www.fmrib.ox.ac.uk/fsl/) and PET and MRI images were spatially transformed relative to the standard MNI atlas. Regional tissue uptake of $H_2{}^{15}O$ was globally normalized to whole brain rCBF mean value with images scaled to a mean of 1,000 counts. These value and spatially normalized images were tri-linearly interpolated, re-sampled (60 slices, 8 mm^3 voxels), and Gaussian filtered to a final resolution of 9.9 mm (Full Width at Half Maximum).

2.4.2. MRI

MRI data from the two groups were preprocessed in the same manner. The initial 3 volumes of the fMRI data were discarded and the remaining volumes acquired when fMRI signals were in steady-state were further analyzed. The DICOM images were converted to the NIFTI format using the Multi-image Analysis GUI (Mango) (ric.uthscsa.edu/mango/). Structural images were stripped of the cranial and outer visceral layers using the Brain Extraction Tool (BET) plug-in within Mango (Smith, 2002). Both functional and structural images were visually inspected to look for major movement artifacts and usability of data and removed from the study as necessary.

Individual fMRI data processing was carried out using FSL (FMRIB Software Library; http://fsl.fmrib.ox.ac.uk/fsl/) (Smith et al., 2004), and the following pre-statistics processing were applied: motion correction (Jenkinson et al., 2002), slice-timing correction using Fourier-space time-series phase-shifting, removal of non-brain structures (Woolrich et al., 2001), spatial smoothing using a Gaussian kernel of 5 mm with grand-mean intensity normalization of the entire 4D dataset by a single multiplicative factor, high-pass temporal filtering (Gaussian-weighted least-squares straight line fitting, with sigma = 30.0 s).

2.5. Data processing

2.5.1. PET

Further data analyses were performed using MIPS software (Multiple Image Processing Station, Research Imaging Institute, UT Health Science Center at San Antonio, TX) and MANGO (Multi Analysis GUI, ric.uthscsa.edu/mango). For each subject, voxel-by-voxel pairwise contrast was generated contrasting reading versus rest to identify regional CBF changes present during reading. Within-subject regional changes were then averaged across the subjects. A maxima and minima search was then used to identify local extrema within a search volume measuring 1000 cubic mm (Fox et al., 1988; Fox and Mintun, 1989; Mintun et al., 1989). A gamma 1 statistic measuring skewness and gamma 2 statistic measuring kurtosis of the distribution of the extrema established before post hoc analysis were used as an omnibus test to assess overall significance. The group-mean subtraction image was then converted to statistical parametric images of z scores (SPI{z}). Brain regions with increases in CBF with z score > 3, p > 0.005 (false discovery rate corrected q = 0.05), and cluster size > 80 mm^3 are reported.

2.5.2. MRI

fMRI data were processed using FEAT (FMRI Expert Analysis Tool) Version 6.00 part of FSL (Worsley, 2001), by fitting a general linear model to determine differences in activation profiles during reading and rest conditions, on an individual basis and across subjects (grouped by participant type) using FLAME (FMRIB's Local Analysis of Mixed Effects) stage 1 (Beckmann et al., 2003; Woolrich et al., 2004; Woolrich, 2008). For fMRI data processing, Z (Gaussianised T/F) statistic images were thresholded using clusters determined by Z > 2.3 and a (corrected) cluster significance threshold of P = 0.05 (Woolrich et al., 2004). Cluster size > 125 mm^3 are reported.

For both MRI and PET, the images were displayed and significant clusters were labeled in MNI coordinates of Brodmann areas (BA) using MANGO (Multi Analysis GUI, ric.uthscsa.edu/mango).

2.6. Comparison between PET and MRI derived speech production networks

The PET and fMRI derived SPN in typical speakers and speakers with HKD were examined for spatial similarity by using a Pearson spatial crosscorrelation measure (FSL, www.fmrib.ox.ac.uk/fsl/). We applied Fisher's r-to-z transform using a conservative degrees-of-freedom value of 500 (number of independent resolution elements Smith et al., 2009) and converted the resulting z score to a P value. Additionally, in order to examine if the new overt speech paradigm can be used to detect alterations in the neural control system for speech in speakers with HKD, the PET and fMRI derived SPN for typical speakers were contrasted against those derived for speakers with HKD using the processing methods described above.

3. Results

3.1. Speech and voice characteristics

3.1.1. Typical speakers

While typical speakers were not evaluated by a SLP, they were screened for history of speech and language disorders. All participants had normal hearing. Their detailed demographics are listed in Table 1.

3.1.2. Hypokinetic dysarthria

The diagnosis of PD was confirmed in all participants. Their detailed demographics and clinical characteristics are listed in Table 1. The PET cohort was younger than the fMRI cohort (p = 0.03), although most individuals in the two groups were between 50 and 70 years (80% of PET cohort and 55% of fMRI cohort). There was no significant difference between the PET and the fMRI groups for clinical parameters of PD

Table 1
Demographics of Typical Speakers and Speakers with Hypokinetic Dysarthria.

	Typical Speakers	Speakers with HKD-PET study	Speakers with HKD-fMRI study	p value
Number	19	10	21	–
Age (years)	29.3 ± 9	60 ± 11	69 ± 9	0.03
Range (years)	21–50	40–82	50–79	–
Handedness: R/L/Ambi	19/0/0	10/0/0	18/2/1	0.9*
Gender: Male/Female	9/10	8/2	13/8	0.4*
IPD duration (years)	NA	4.1 ± 1.6	6.7 ± 4.8	0.1
UPDRS Score (items 5–31) on medication	NA	51 ± 12	43 ± 15	0.1
Reported speech symptoms (UPDRS item 5)	NA	2.2 ± 0.4	1.8 ± 0.7	0.1
Speech motor examination (UPDRS item 18)	NA	1.9 ± 0.7	1.7 ± 0.5	0.3
Hahn & Yahr stage	NA	2.5 ± 0.4	2.6 ± 0.7	0.6
Vocal intensity during reading (dB SPL)	NA	68 ± 2	66 ± 4	0.1
HKD severity	NA	moderate to severe	moderate to severe	–

R: right; L: left; Ambi: ambidextrous. NA: not applicable. UPDRS: Unified Parkinson's Disease Rating Scale.
Hoehn & Yahr Staging of Parkinson's Disease, Stage 0 = no signs of disease, Stage 1 = Mild symptoms, Stage 2 = Bilateral involvement without impairment, Stage 3 = mild to moderate bilateral disease, Stage 4 = severe disability, Stage 5 = wheelchair bound or bedridden.
SPL – sound pressure level.
*chi-square test.

duration, UPDRS scores (total, items 5 and 18), and Hahn & Yahr stage (see Table 1). On average, both cohorts rated their speech intelligibility to be moderately affected (UPDRS item 5), because they were sometimes asked to repeat their statements. Clinicians rated speech on UPDRS item 18 to be mild with slight loss of expression, diction and/or volume in 30% of speakers with HKD. Speech was rated to be moderately impaired (monotone, slurred but understandable) in 50% of PET cohort and 70% of fMRI cohort. Only 20% PET cohort were found to have speech that was difficult to understand. The severity of HKD and the level of hypophonia were not significantly different between the two groups. Individuals in each group were rated qualitatively by an SLP with more than 20 years of experience in evaluating and treating disorders of speech motor control. Patients were deemed have moderate to severe speech and voice characteristics associate with HKD. For example, individuals with dysfluencies, moderate degree of imprecise articulation, reduced variability in pitch and loudness, and breathy voice were rated to have moderate HKD, while persons with marked dysfluency, severely imprecise articulation, accelerated speech rate, little or no variation in pitch and loudness, and greatly reduced range of articulatory movement were deemed to have severe HKD. While intelligibility was not specifically evaluated, SLPs did not deem any speaker with HKD to be unintelligible. The vocal intensity measured during reading the Rainbow Passage in the PET and fMRI cohorts were 68 ± 2 and 66 ± 4 dB sound pressure level (SPL) measured with a microphone at 50 cm distance. However, all patients were able to increase vocal loudness by at least 5 dB on command.

3.2. PET

3.2.1. Typical speakers

The conditional contrast between reading and rest identified brain areas engaged during overt speech production in the cohort of typical speakers (Table 2, Fig. 1). Brain regions showing significant activation and their peak extrema are detailed in Table 2. Activations in the supplementary motor cortex (SMA), dorsal premotor cortex (PMd, BA 6), anterior cingulate gyrus (BA 32), primary motor cortex (M1-mouth/larynx, BA 4), pars opercularis (BA 44), transverse temporal sulcus (BA 41) and superior temporal gyrus (BA 21/22) were noted bilaterally. Activations in the visual cortex (cuneus, BA 17 and lingual gyrus, BA 18) and cerebellum (lobules IV, VI, VIIIA and VIIB) were bilateral while the putamen activation was found to be left lateralized.

3.2.2. Speakers with HKD

The overt speech task in individuals with PD with symptoms of HKD also engaged the same regions noted in typical speakers (Table 3, Fig. 2). Brain regions showing significant activation and their peak extrema are detailed in Table 3. The activations in the M1-mouth/larynx, SMA, PMd were found to be smaller in the left hemisphere and almost absent in the right hemisphere when compared to typical speakers. Activations in the visual areas and cerebellum were found to be similar in extent to the typical speakers (See Fig. 2). Activations in putamen and thalamus were observed bilaterally, but did not remain significant after correction for multiple comparisons.

3.3. Functional MRI

3.3.1. Motion correction parameters

Head motion has been a major concern in functional connectivity of speech production tasks. Therefore, we examined the motion correction parameters of the fMRI images since one of the primary concerns of performing connected speech production tasks in MRI is the decrement in the image quality resulting from head motion. In both our cohorts, the head translation and rotation while overtly and continuously speaking was small and was not significantly different ($p > 0.4$) between the two groups. The average absolute translation in both groups was found to be 0.12 mm with the maximum translation being 0.4 mm (See Table 4 for additional details). All participants performed the task appropriately, and data from all participants were included in the analysis.

3.3.2. Typical speakers

The SPN identified in the cohort of typical speakers using the new overt connected speech paradigm was consistent with the PET-derived SPN map (Table 2, Fig. 3). The brain areas, their BA label, the x, y, and z coordinates, and the z scores are detailed in Table 2. Activations were observed bilaterally in M1-mouth, SMA, PMd, opercular postcentral gyrus (BA 43), transverse temporal gyrus, and superior and middle temporal gyri. Similar to the observed findings in PET, bilateral activations were noted in putamen, visual areas and cerebellum. Additional activation in the left cingulate cortex (BA 24) was observed (See Table 2 and Fig. 3) in this group.

3.3.3. Speakers with HKD

The brain areas, their BA label, the x, y, and z coordinates, and the z scores are detailed in Table 3. As was observed in the PET study in another cohort with HKD, fMRI using overt connected speech task in speakers with HKD also identified activations in M1-mouth, SMA, and PMd that were of smaller volume in both hemispheres when compared to typical speakers (Table 3, Fig. 4). The activation in the bilateral temporal lobes were found to be of greater volume than seen in PET but

Table 2
Regions of the speech motor network activated during a paragraph reading task in Typical Speakers mapped by PET and fMRI.

			PET				fMRI			
Lobe	Location	Brodmann area	x	y	z	Z score	x	y	z	Z score
Frontal	Precentral gyrus (M1 mouth)	4	−50	−10	40	10.3	−56	−6	42	5.8
	Precentral gyrus	6	−52	−8	34	9.2	−52	−10	28	5.3
	Precentral gyrus	6					−52	2	48	5.2
	Pars opercularis/Precentral gyrus	44	−52	4	4	5.1				
	Medial frontal gyrus (SMA)	6	−12	−12	60	4.6	−2	6	42	4.9
	Cingulate gyrus	24					−16	10	34	4.6
	Medial frontal gyrus (SMA)	6	0	0	62	7.7	6	6	64	5.2
	Cingulate gyrus	32	10	12	42	3.8				
	Precentral gyrus (M1 mouth)	4	56	−6	38	6.9	54	−8	32	5.7
	Precentral gyrus	6	52	−4	38	5.9	56	−2	42	5.5
	Pars opercularis/Precentral gyrus	44	52	14	4	3.4				
	Precentral gyrus	43					58	−4	8	4.7
	Subcallosal gyrus	25	8	12	−20	3.6				
Temporal	Superior temporal gyrus	22	−62	−30	2	3.7	−64	−18	−2	6.2
	Middle temporal gyrus	22					−56	−42	6	4.6
	Transverse temporal gyrus	41	−56	−18	10	5.4				
	Superior temporal gyrus	41	52	−36	12	3.4	50	−30	2	5.1
	Superior temporal gyrus	42	68	–22	6	3.5				
	Superior temporal gyrus	22	62	−6	0	4.8	66	−26	2	5.2
	Transverse temporal gyrus	41	46	−24	10	4.2				
Parietal	Postcentral gyrus	43	−56	−4	16	4.2	−58	−4	16	5.1
	Superior parietal lobule	7	−24	−62	52	4.3				
	Postcentral gyrus	43	60	−6	20	5.6	56	−6	18	5.8
	Precuneus	7	18	−42	52	3.8				
Subcortical	Insula	13	–32	−38	18	4.4				
	Insula	13	−40	10	6	3.6				
	Claustrum/insula	13	−30	8	12	3.9	−28	22	12	5
	Insula	13	44	6	6	3.5				
	Lentiform Nucleus-Putamen						22	14	12	5.0
Occipital	Cuneus	17	−12	−96	8	7.4				
	Lingual gyrus	17					−2	−96	−2	6.1
	Lingual gyrus	18	−2	90	0	7.1	−6	−84	−2	5.5
	Lingual gyrus	18	4	−84	−2	8.1	8	−80	0	6.2
	Lingual gyrus	17					10	−98	2	6.1
Cerebellum	Culmen	lobule VI	–22	−58	−26	7.4	–22	−62	–22	5.6
	Declive	lobule VI					−12	−62	−18	5.3
	Inferior semi-lunar lobule	lobule VIIIA/B	−8	−68	−44	4.9	−8	−72	−38	4.3
	Declive	lobule VI	18	−64	−16	7.1	16	−66	–22	5.3
	Culmen	lobule IV	12	−40	−30	4.2	26	−56	−26	5.4
	Inferior semi-lunar lobule	lobule VIIB	10	−70	−42	3.7	12	−70	−40	5.3

Locations of peak extrema (x, y z in MNI coordinates).

still smaller than that seen in typical speakers. The activations in the visual cortex and cerebellum were similar to that noted in other HKD group and typical speakers. Additional activations in left pre-SMA, bilateral thalami (medial dorsal nucleus), and bilateral parietal lobe (precuneus, BA 7) were noted in this cohort (See Table 3, Fig. 4). Activation in left putamen did not remain significant after correction for multiple comparisons.

3.4. Comparison between PET and MRI derived speech production network

The cross-correlation analysis found that the SPN derived from PET and fMRI demonstrated significant spatial overlap ($p < 0.001$) in both typical speakers and speakers with HKD (See Table 5 for r values). The SPN within modality (i.e. PET in typical speakers and speakers with HKD and fMRI in typical speakers and speakers with HKD) had the highest correlation (0.55 for PET and 0.54 for MRI). The spatial overlap between the PET and fMRI derived SPN in typical speakers had a r value of 0.52 and is shown in Fig. 5, panel A. The PET SPN had more activity in SMA, primary auditory cortex (BA 41), and visual cortices, while fMRI SPN showed more activation in secondary auditory cortices (BA 21/22). The spatial overlap between the PET and fMRI derived SPN in speakers with HKD had a r value of 0.43 and is shown in Fig. 5, panel B. SPN identified by fMRI in speakers with HKD showed more activation in precuneus, temporal lobes and cerebellum.

Using the overt speech production paradigm in PET, we found that when compared to typical speakers, speakers with HKD had decreased activity in bilateral dorsal premotor and motor and auditory cortices (Figs. 6 and 7, panel A). Speakers with HKD demonstrated greater activity in left inferior parietal lobule (BA 40) during overt speaking. Similar to the findings in PET, fMRI using the overt speech paradigm also identified significant reductions in activity in dorsal premotor and primary motor cortices and operculum (BA 43) and increased activity in left BA 40 in speakers with HKD. Additionally, speakers with HKD demonstrated significantly decreased activity in the left M1 mouth/larynx (Figs. 6 and 7, panel B). The decreased activity in the temporal lobe of speakers with HKD was more evident in PET. Further, it was found to be reduced in fMRI in those analyses that ignored cross subject and random effects variance (i.e., fixed effects analysis) but did not remain significant when these variances were modeled (i.e., mixed effects analysis). The brain areas, their BA label, the x, y, and z coordinates, and the z scores are detailed in Table 6.

4. Discussion

In this study, SPNs were obtained by fMRI using an overt continuous speech paradigm and were compared to the SPN identified by PET in a large cohort of typical speakers. The fMRI overt connected speech paradigm did not result in excessive motion artifacts and, consistent

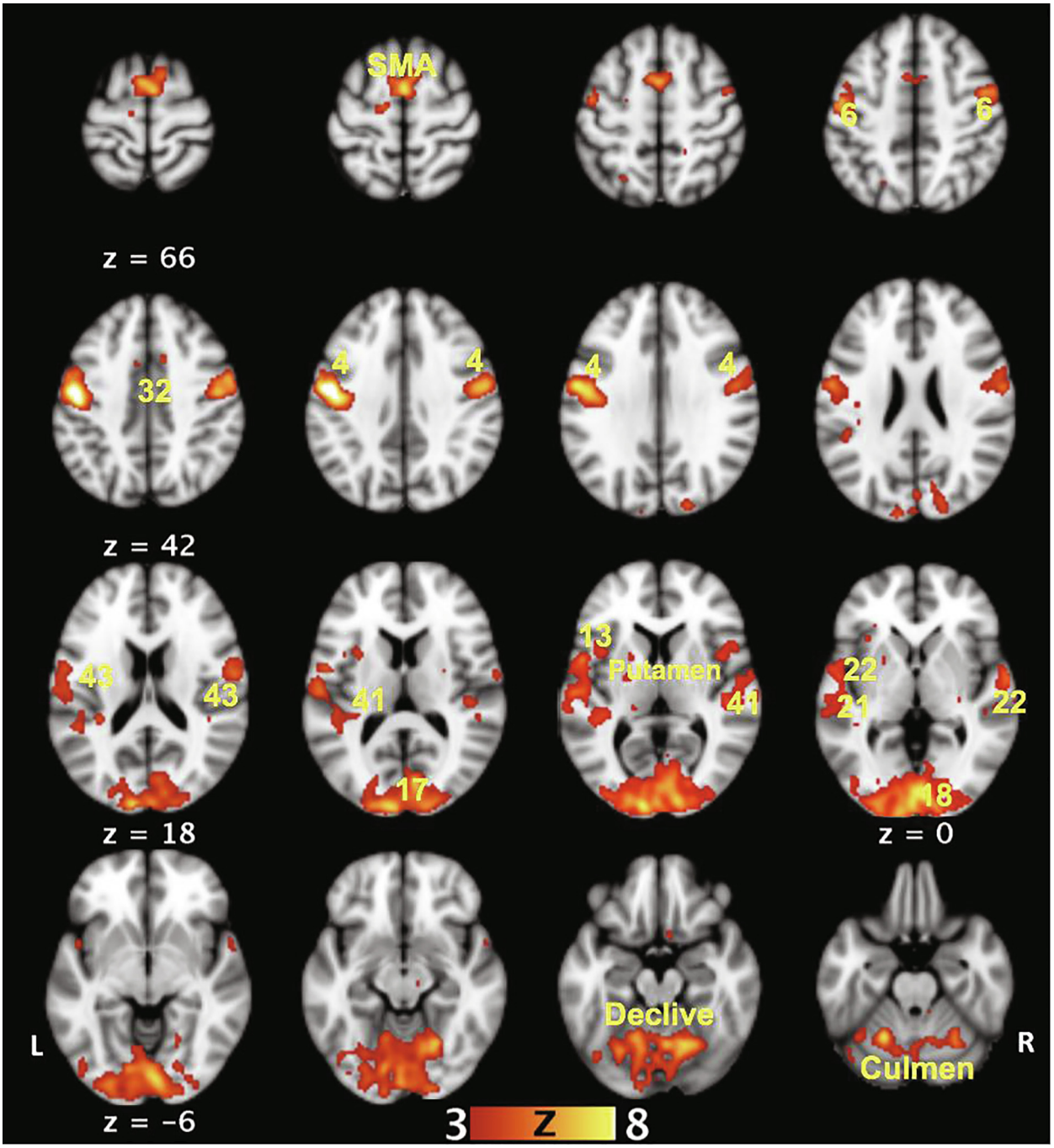

Fig. 1. Speech motor areas engaged during reading aloud in the cohort of typical speakers identified by PET. The activation map is overlaid on the MNI template and the standard z coordinates are listed below the axial slices. The left hemisphere is on the left side of the image. The Brodmann areas are numbered: 6 - Dorsal premotor cortex, 32 – Cingulate gyrus, 4 - Primary motor cortex (M1-mouth), 43 – Precentral gyrus, 41 – Transverse temporal gyrus, 13 – Insula, 21 and 22 – Superior temporal gyrus, 17 – Cuneus, 18 – Lingual gyrus. In addition, the supplementary motor area (SMA) and the declive and culmen areas of the cerebellum are identified.

with our expectations, successfully identified the same brain areas demonstrated in a PET study using the same paradigm in these individuals. The SPNs derived in this cohort from PET and fMRI demonstrated significant spatial overlap ($r = 0.52$; $p < 0.001$, Table 5) and identified brain areas belonging to the feedforward subsystem (SMA, PMd, anterior cingulate cortex, putamen, M1-mouth/larynx, cerebellum) and the feedback subsystem (primary and secondary auditory areas in the temporal lobe) in both hemispheres (Tables 2 and 4, Figs. 1, 2, and 5).

As an additional validation, we used the new overt continuous speech paradigm to map the SPN in individuals with HKD secondary to PD and compared the results with the SPN identified in an earlier PET study using the overt speaking paradigm in another cohort of individuals with PD having HKD (Narayana et al., 2010). Similar to what we found in typical speakers, the SPN derived from the new fMRI paradigm closely matched that obtained by PET in speakers with HKD ($r = 0.43$; $p < 0.001$, Table 5). Consistent with our previous findings in PET, the fMRI paradigm identified activations in M1-mouth, SMA, and PMd primarily in the left hemisphere (Table 4, Figs. 3–5) and decreased engagement of right hemisphere regions during speech production in speakers with HKD.

This study also compared the SPN of speakers with HKD and typical

Table 3
Regions of the speech motor network activated during a paragraph reading task in speakers with HKD mapped by PET and fMRI.

			PET				fMRI			
Lobe	Location	Brodmann area	x	y	z	Z score	x	y	z	Z score
Frontal	Precentral gyrus (M1-mouth)	4	−46	−14	42	4.9	−52	−8	48	4.8
	Precentral gyrus	4	−62	0	22	3.4	−58	−6	20	4.1
	Precentral gyrus	6	−46	−2	48	6.8	−46	4	48	5.03
	Medial frontal gyrus (SMA)	6	−6	0	68	5.7	−10	4	66	5.8
	Medial frontal gyrus (Pre-SMA)	6	−4	16	50	3.7	−2	12	66	5.7
	Cingulate cortex	24	−10	20	32	3.5				
	Cingulate cortex	32					−10	14	40	4.1
	Pars opercularis/Precentral gyrus	44	−48	6	8	3.2				
	Precentral gyrus (M1-mouth)	4					50	−8	42	4.3
	Precentral gyrus	6	50	−2	38	3.9	60	−4	30	4.8
	Pars opercularis/Precentral gyrus	44					52	14	6	4.3
	Superior frontal gyrus (pre-SMA)	6					6	12	52	4.5
	Middle frontal gyrus	46					44	16	26	4.8
	Middle frontal gyrus	6					50	4	44	4.7
	Cingulate gyrus	32					8	20	42	4.3
	Medial frontal gyrus (SMA)	6	2	6	60	4.4				
Temporal	Superior temporal gyrus	22	−54	12	−8	3.9	−62	−14	4	5.1
	Middle temporal gyrus	21	−48	–32	−4	3.2	−54	−24	−2	4
	Superior temporal gyrus	41					56	−18	6	4.95
	Superior temporal gyrus	22					58	−26	0	5.2
	Middle temporal gyrus	21					52	−24	−6	4.99
Parietal	Superior parietal lobule	7					−30	−58	50	6
	Precuneus	7	24	−70	54	3.3	28	−66	42	4.9
Subcortical	Insula	13	−40	18	8	3.1				
	Thalamus						−12	−16	4	4.4
	Thalamus						12	−14	4	4.7
Occipital	Lingual gyrus	18	−2	−86	−4	7.3	−6	−84	−12	5.8
	Fusiform gurus	18	–22	−96	−8	9.3				
	Middle/inferior occipital gyrus	18	−26	92	2	6.5				
	Fusiform gurus	37	−48	−66	−14	4.7				
	Cuneus	18					−16	−102	2	5.5
	Cuneus	18					18	−100	2	5.4
	Lingual gyrus	17/18	2	−86	0	7.5	6	−80	0	5.7
	Lingual gyrus	17	22	−96	0	6.6	14	−94	−12	5.8
Cerebellum	Declive	lobule VI	−16	−72	−20	4.9	−28	−64	–22	5.5
	Culmen	lobule IV/V	−30	−50	−24	4.5				
	Inferior semilunar lobule		−24	−70	−40	4.5				
	Declive	lobule VI	12	−68	−18	6.6				
	Culmen	lobule IV/V	28	−62	−24	5.2	26	−64	−24	5.6
	Inferior semilunar lobule		12	−76	−40	4				
	Declive	Crus I					36	−74	–22	4.5

Locations of peak extrema (x, y z in MNI coordinates).

speakers derived by the two modalities, PET and fMRI. Such an intra-individual comparison of the mapping of SPN network by these two modalities has not been previously reported. Consistent with our hypothesis, we replicated the changes in speech motor areas in HKD previously observed in the PET studies (Liotti et al., 2003; Pinto et al., 2004) and, for the first time, demonstrated that these alterations could also be identified using the new overt speech paradigm in fMRI (Table 6, Figs. 6 and 7). Indeed, both imaging methods demonstrated that when compared to typical speakers, speakers with HKD have significantly decreased activity in critical feedforward (bilateral dorsal premotor and motor cortices) and feedback (auditory and somatosensory areas) subsystems.

The findings from this study have demonstrated that the overt connected speech paradigm is feasible in fMRI. By limiting the movement of jaw and lips, the paradigm greatly reduced the speech related head movements as demonstrated by very small translations during scanning (Table 3). The overt reading task was not exactly matched between PET and fMRI. In PET, the mask was a physical barrier that limited the jaw movement while in fMRI, the participants had to consciously limit their jaw movements. During the fMRI practice session we found that the participants were able to read aloud while voluntarily closing their jaws without any difficulty and since each fMRI reading epoch was for only 30 s, the participants were able to do this task without fatigue. Absence of excessive motion during fMRI indicates that the participants were complaint with the task. Another important aspect to consider is differential activation patterns in the sensorimotor cortex arising from the additional orofacial movements in one imaging method versus the other. Although a dorso-ventral somatotopic organization of the lips, jaw, larynx, and tongue has been demonstrated (Penfield and Rasmussen, 1950; Brown et al., 2009; Grabski et al., 2012), at a group level, the peak activations for lips, jaw and tongue are embedded within the larger activation seen in the primary motor cortex and operculum in speech tasks. In typical speakers, the activation in bilateral sensorimotor cortices noted in PET and fMRI was found to have a high degree of overlap (Fig. 5, panel A). Therefore we believe that the differences in task performance between PET and fMRI are small and do not contribute to significant differences in activation patterns between the two modalities.

We have also demonstrated that this task was feasible even in individuals with movement disorders such as PD. The task did not require extensive training or practice. Further, all participants in this study were able to reliably speak with closed jaw and lips after only 2–3 trials and successfully completed the task in the MRI scanner. The activation map derived using the new fMRI paradigm was validated against the 'gold standard' – the PET derived activation map in the same individuals. Therefore, we believe that SPN can be reliably mapped using the new fMRI overt speech paradigm. This paradigm will be especially useful in studying motor speech and voice disorders, including

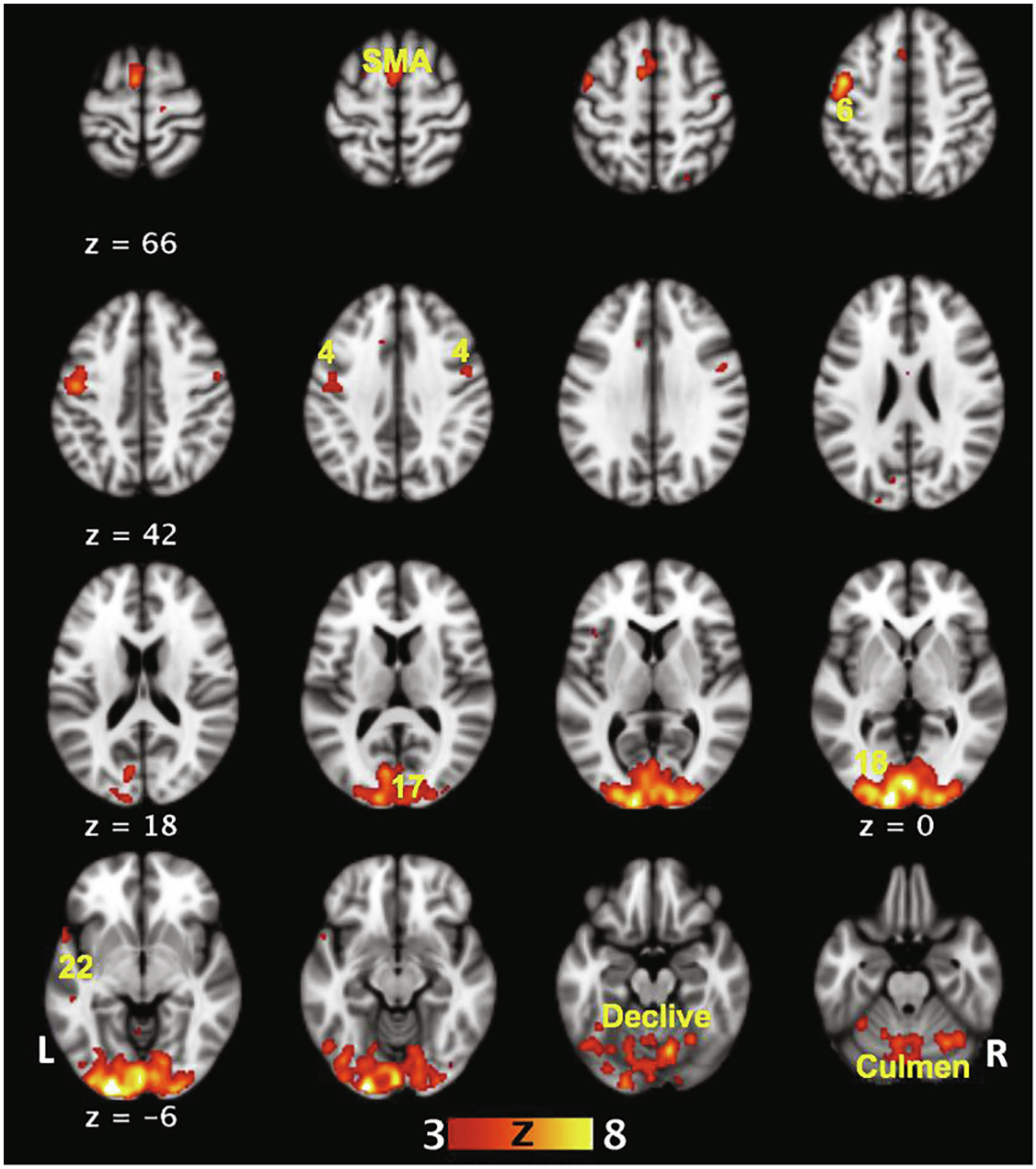

Fig. 2. Speech motor areas engaged during reading aloud in the cohort of speakers with Hypokinetic dysarthria identified by PET. The activation map is overlaid on the MNI template and the standard z coordinates are listed below the axial slices. The left hemisphere is on the left side of the image. The Brodmann areas are numbered: 6 - Dorsal premotor cortex, 4 - Primary motor cortex (M1-mouth), 22 – Superior temporal gyrus, 17 – Cuneus, 18 – Lingual gyrus. In addition, the supplementary motor area (SMA) and the declive and culmen areas of the cerebellum are identified.

Table 4
Motion correction parameters during fMRI overt paragraph reading task in typical speakers and speakers with HKD.

	Absolute Translation (mm)	Relative Translation (mm)	Rotation (radians)
Typical Speakers	0.12 ± 0.04	0.11 ± 0.02	0.002 ± 0.001
Speakers with HKD	0.12 ± 0.08	0.07 ± 0.05	0.003 ± 0.006

stuttering, apraxia of speech, dysarthria, and spasmodic dysphonia. This paradigm could also be used more widely for mapping SPNs in populations for which PET carries higher risk (e.g. children), in studies where PET may be cost-prohibitive, or to reduce the scanning duration in studies currently using an event-related fMRI paradigm. Furthermore, the high signal-to-noise ratio inherent in block-design fMRI allows this paradigm to be applied for mapping at the individual level, which is critical in presurgical functional mapping or for identifying regions to target using TMS.

The SPN mapped by the new fMRI paradigm in typical speakers is not only consistent with the map derived from PET in the same individuals, it is also consistent with published PET and fMRI studies of speech production (Brown et al., 2009; Guenther, 2016; Price, 2010, 2012) and their *meta*-analyses (Turkeltaub et al., 2002; Brown et al., 2005; Brown et al., 2009). This new overt speech paradigm in typical speakers identified brain areas included in the feedforward and feedback subsystems within the framework of the Directions into Velocities of Articulators (DIVA) model of speech motor control (Guenther, 2016). The dorsal premotor cortex, SMA, insula, cingulate cortex, and articulatory and laryngeal M1 cortices, along with putamen and cerebellum,

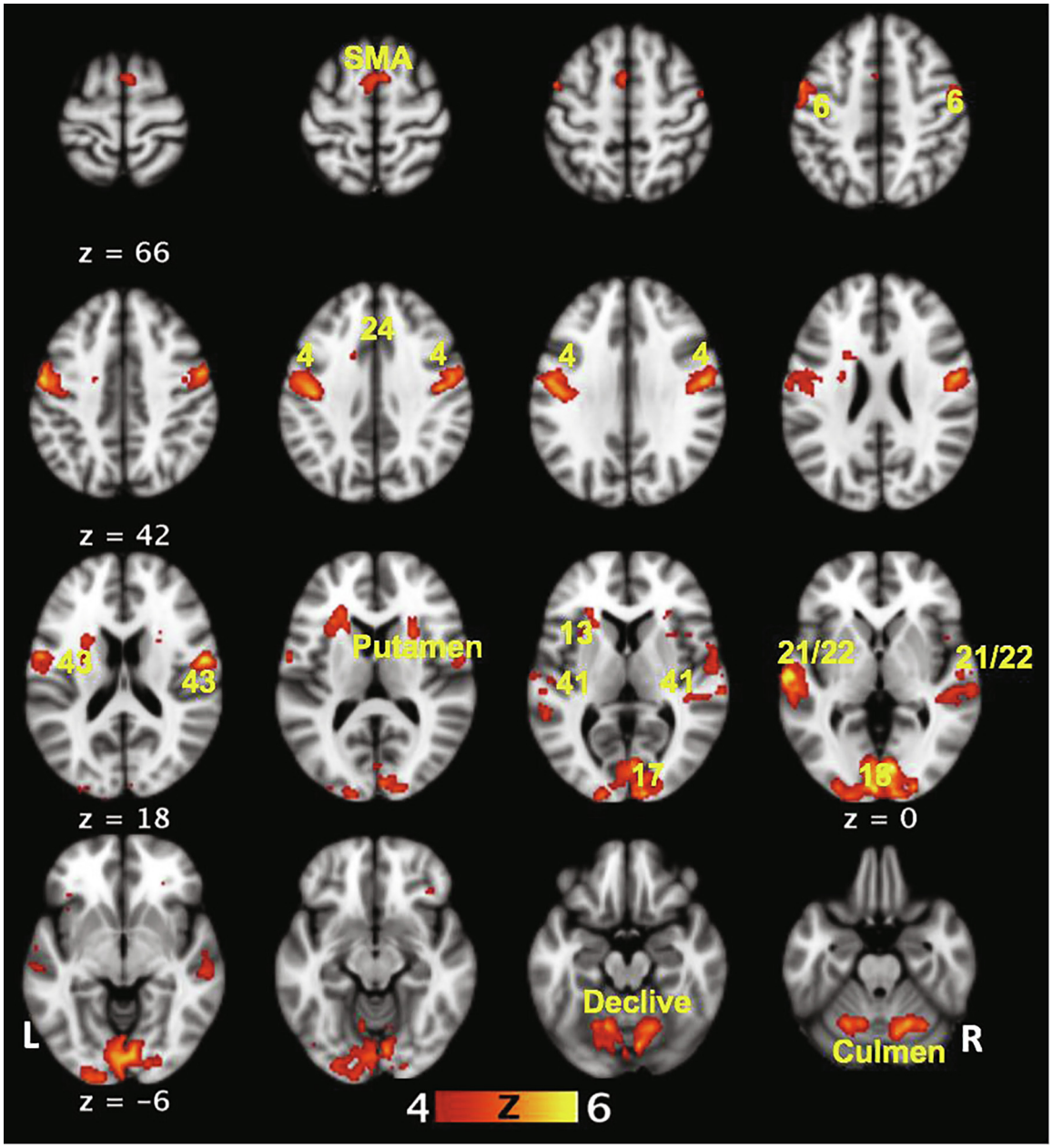

Fig. 3. Activation pattern detected using BOLD fMRI using the overt connected speech paradigm in healthy individuals. The activation map is overlaid on the MNI template and the standard z coordinates are listed below the axial slices. The left hemisphere is on the left side of the image. The Brodmann areas are numbered: 6 - Dorsal premotor cortex, 24 – Cingulate gyrus, 4 - Primary motor cortex (M1-mouth), 43 – Post central gyrus, 41 – Transverse temporal gyrus, 13 – Insula, 21 and 22 – Superior temporal gyrus, 17 – Cuneus, 18 – Lingual gyrus. In addition, the supplementary motor area (SMA) and the declive and culmen areas of the cerebellum are identified.

that are included in the feedforward subsystem were identified in our cohort. These areas mediate speech initiation, speech sound map, and articulation including control of orofacial and laryngeal muscles and breathing. Components of feedback subsystem that monitor auditory (primary and secondary auditory cortices) and somatosensory input (ventral somatosensory cortex, BA 43) and feedback control area of ventral premotor cortex in the right hemisphere were also found to be activated during overt continuous speech. Furthermore, all key brain areas for the control of phonation during speaking (Brown et al., 2009) were found to be activated using the new overt connected speech task in fMRI. This provided further evidence for the engagement of M1-larynx during speech production and indicated that this task can be used to study phonatory processes in healthy and diseased states. Finally, this paradigm also identified significant activation in the superior temporal sulcus in the right hemisphere, which has been shown to play a role in maintaining short-term memory of speech sounds, spectral-temporal processing of auditory input, and integrating auditory feedback during speech production (Seghier et al., 2015; Yamamoto et al., 2019). As expected, we did not see significant activations in brain areas monitoring semantic and linguistic features during spontaneous speech or reading novel material.

We also observed some differences in the SPN regions identified by PET and fMRI in typical speakers. For instance activations in BA 44 and insula were noted in PET but not in fMRI. Activations BA 44 in the left hemisphere and insula in both hemispheres did not survive the z-score significance threshold (Left BA 44: MNI co-ordinates −46, 12, 4, z-score = 3.5; left insula: MNI co-ordinates −40, 10, 8, z-score = 3.9; right insula: MNI co-ordinates 42, 18, 6, z-score = 2.3). Future studies

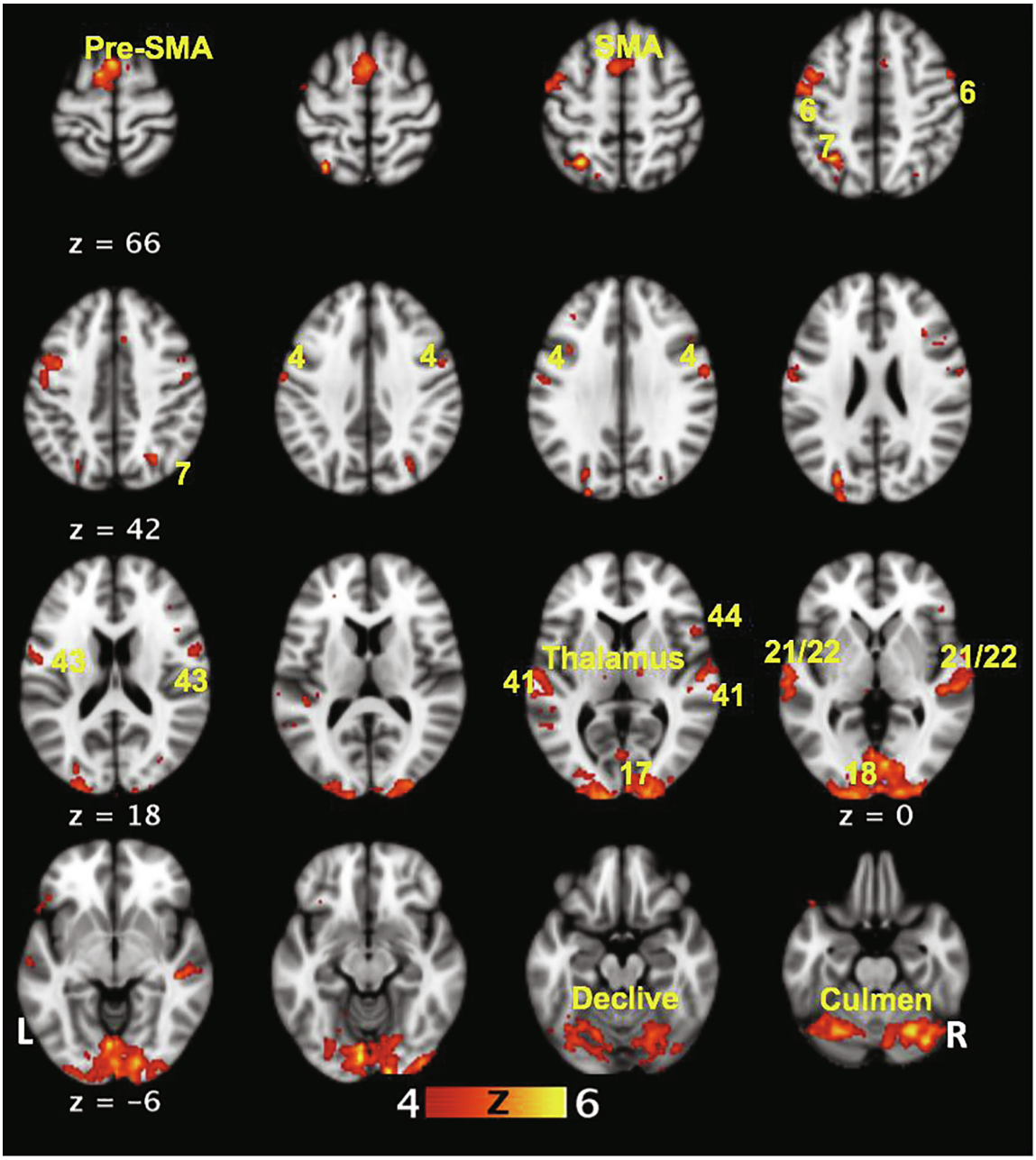

Fig. 4. Activation pattern detected using BOLD fMRI using the overt connected speech paradigm in speakers with HKD. The activation map is overlaid on the MNI template and the standard z coordinates are listed below the axial slices. The left hemisphere is on the left side of the image. The Brodmann areas are numbered: 6 - Dorsal premotor cortex, 7 – Precuneus, 4 - Primary motor cortex (M1-mouth), 43 – Post central gyrus, 41 – Transverse temporal gyrus, 13 – Insula, 21 and 22 – Superior temporal gyrus, 17 – Cuneus, 18 – Lingual gyrus. In addition, activation in right inferior frontal gyrus (BA 44), pre-SMA, SMA, and declive and culmen areas of the cerebellum are identified.

should further investigate the ideal threshold for interpreting fMRI results. In the temporal lobe, auditory areas BA 41 and 42 were not activated significantly in fMRI. Unlike in PET, the background fMRI machine noise possibly engaged of the primary auditory cortices in a similar manner during rest and task conditions. Importantly, the association auditory cortices critical in auditory feedback during speech were observed in both fMRI and PET. Similar differences were found between the SPN regions identified by PET and fMRI in the HKD cohort. Once again the significance level thresholding and different patient groups studied by the two methods likely contributed in these

Table 5
The cross correlation indicating the extent of spatial overlap of speech motor maps derived from PET and fMRI in both typical speakers and speakers with HKD.

	Typical Speakers-fMRI	Speakers with HKD-PET	Speakers with HKD-fMRI
Typical Speakers-PET	0.52	0.55	0.41
Typical Speakers-fMRI		0.42	0.54
Speakers with HKD-PET	0.42		0.43

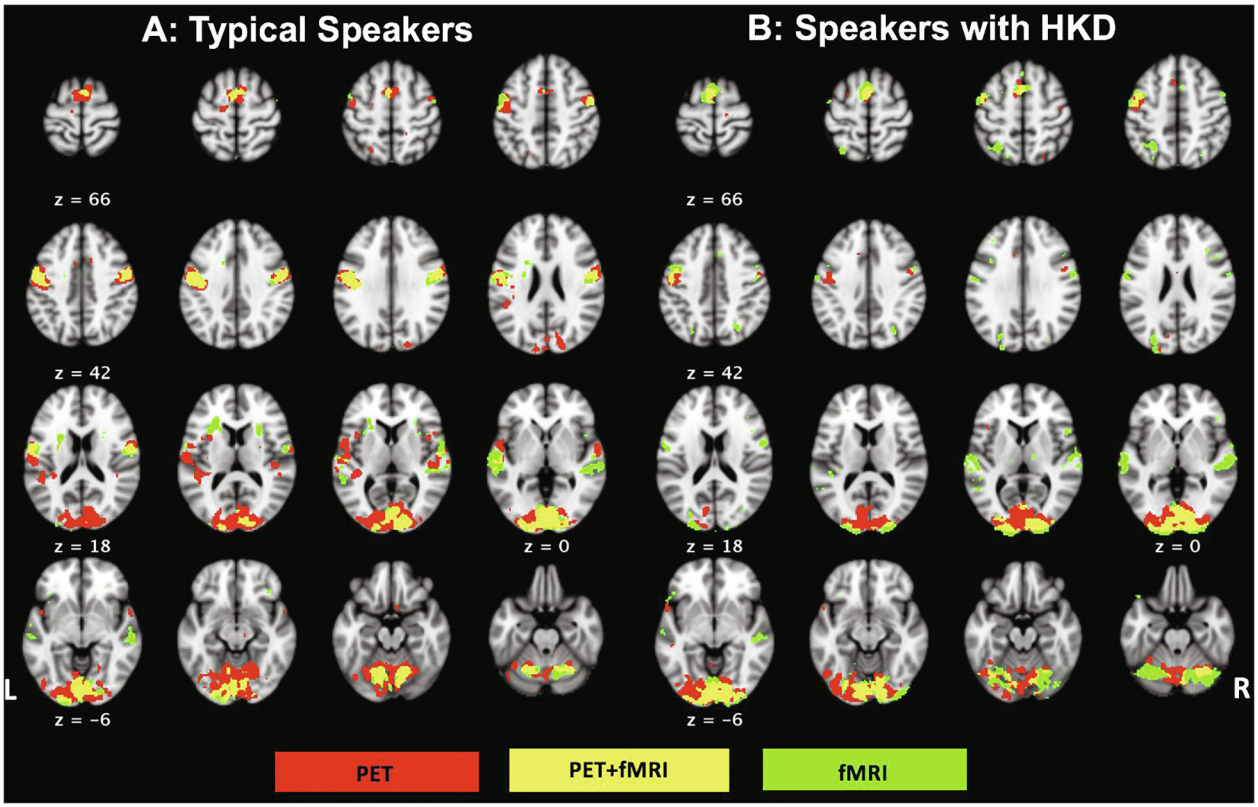

Fig. 5. Speech motor maps in PET and fMRI derived in A. typical speakers and B. Speakers with HKD. The left hemisphere is on the left side of the image. Activation maps in red are from PET and those in green are derived from fMRI. The overlapping activations from the two modalities are shown in yellow. Note significant overlap of activity in the SMA, M1 mouth/larynx, visual cortex and the cerebellum in typical speakers and speakers with HKD. (For interpretation of the references to colour in this figure legend, the reader is referred to the web version of this article.)

differences.

The present study also demonstrated that the new overt connected speech fMRI paradigm can successfully identify disordered SPN in individuals with HKD. It is now established that, in addition to characteristic appendicular motor signs such as tremor, the majority of individuals with PD develop speech and voice disorders (HKD) during their lifetime (Duffy, 2005; Mahler et al., 2015). Speakers with HKD suffer from reduced loudness or hypophonia, poor voice quality, reduced pitch variation, hoarseness, a breathy voice, and imprecise articulation leading to an overall reduction in speech intelligibility (Duffy, 2005). HKD is thought to arise from physiological deficits at laryngeal, articulatory and respiratory apparatus, as well as decreased cortical activity in areas of feedback and feedforward speech motor control systems (Pinto et al., 2004; Narayana et al., 2010; Mahler et al., 2015; Smith et al., 1995; Cannito et al., 2012). Using an overt connected speech production paradigm is ideal for examining the neuronal substrates of these anatomical and physiological abnormalities in HKD since the same connected speech paradigm is used in the clinical evaluation of perceptual and acoustic abnormalities of HKD. Furthermore, the overt speech paradigm is also used to examine the behavioral correlates of pharmacological, behavioral and surgical interventions in clinical evaluations (Brabenec et al., 2019) and therefore the present overt speech approach should be more appropriate to examine the corresponding neural correlates using neuroimaging.

Previous research using overt phonation (Liotti et al., 2003), sentence utterances (Pinto et al., 2004), and paragraph reading (Narayana et al., 2010) in $H_2{}^{15}O$ PET have examined the neural correlates of HKD and the treatment induced changes. When compared to typical speakers, those with PD demonstrated an increased activation in the premotor areas (Pinto et al., 2004; Liotti et al., 2003) with variable of decreases (Pinto et al., 2004) and increases (Liotti et al., 2003) reported in primary motor cortex and cerebellum. Prior fMRI overt speech tasks used in studies of Parkinsonian HKD include phonation (Sachin et al., 2008), diadochokinesis tasks (Riecker et al., 2006), bi- and monosyllabic words (Saxena et al., 2014), sentences (Arnold et al., 2014; Rektorova et al., 2007), freely chosen speech sequence using four possible words (up, down, left and right) (Pinto et al., 2011; Maillet et al., 2012), object naming, and verb generation (Péran et al., 2013). Different patterns of activations in speakers with HKD have been reported across these studies and are different than that reported in the PET studies. For instance, when compared to typical speakers, greater activity in bilateral primary orofacial sensorimotor cortices (Rektorova et al., 2007; Rektorova et al., 2012), left PMd and prefrontal regions (Arnold et al., 2014) as well as a decreased suppression of auditory cortices when processing external auditory feedback (as in hearing one own's voice) has been reported in HKD (Arnold et al., 2014).

Using a connected speech paradigm, our PET study found that when compared to typical speakers, speakers with HKD demonstrated decreased activation in the premotor (PMd and SMA), cerebellum, somatosensory association (BA 43) and auditory cortices (BA 41) in the left hemisphere and primary motor cortex in the right hemisphere (Table 6, Figs. 6 and 7). Speakers with HKD demonstrated greater activity in left inferior parietal lobule (BA 40). The fMRI study also replicated the decreased activity in premotor and somatosensory association cortex (BA 43) and increased activity in left BA 40 in speakers with HKD. Additionally, speakers with HKD demonstrated significantly decreased activity in the left M1 mouth/larynx. Taken together, we interpret these findings to indicate abnormalities in the feedforward and feedback subsystems of SPN in speakers with HKD. We believe that tasks like sustained phonation and isolated sentence reading neither reflect real world behavior nor sufficiently challenge the SPN. Conversely, the connected speech paradigm more closely approximates real

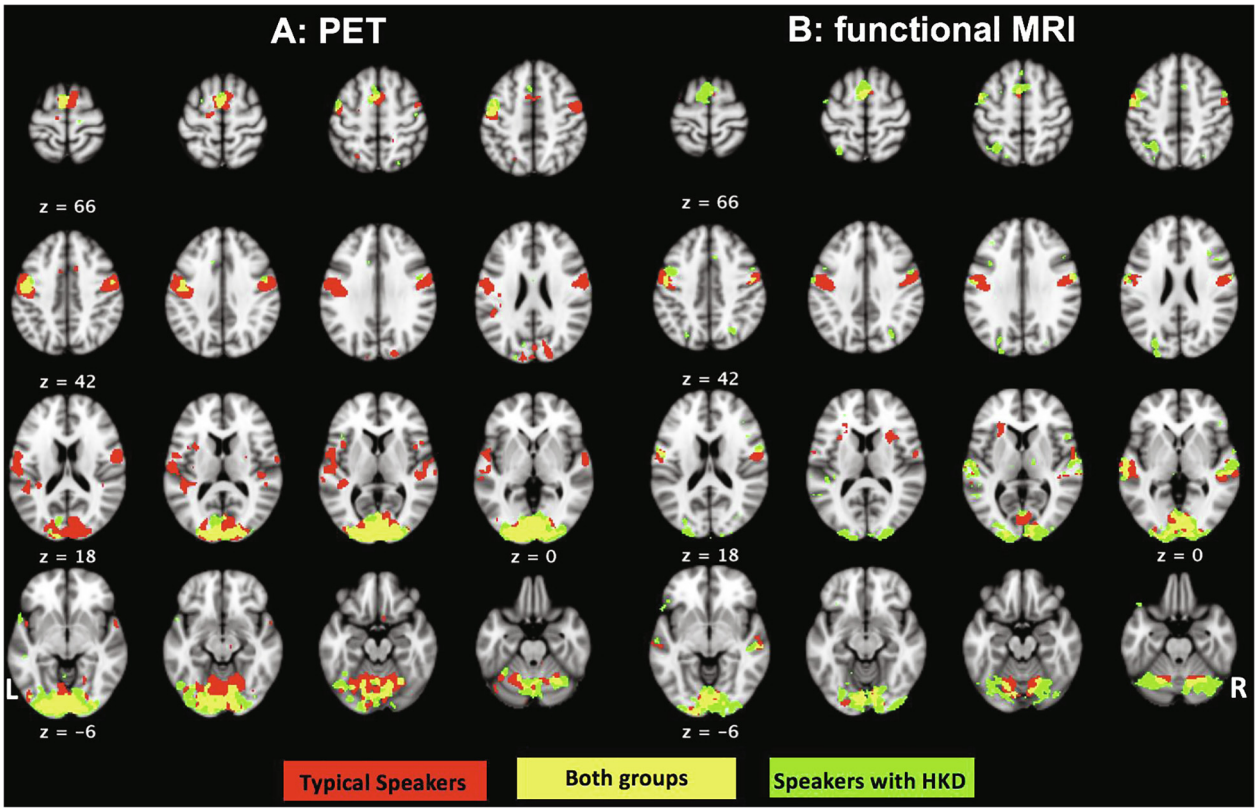

Fig. 6. Speech motor maps in typical speakers and HKD derived by A. PET and B. fMRI. The left hemisphere is on the left side of the image. Activation maps in red are from typical speakers and those in green are in speakers with HKD. The overlapping activations from the two cohorts are shown in yellow. Both PET and fMRI studies found that when compared to typical speakers, speakers with HKD had decreased activity in M1 mouth/larynx and auditory cortex while activity in the visual cortex was of similar extent. (For interpretation of the references to colour in this figure legend, the reader is referred to the web version of this article.)

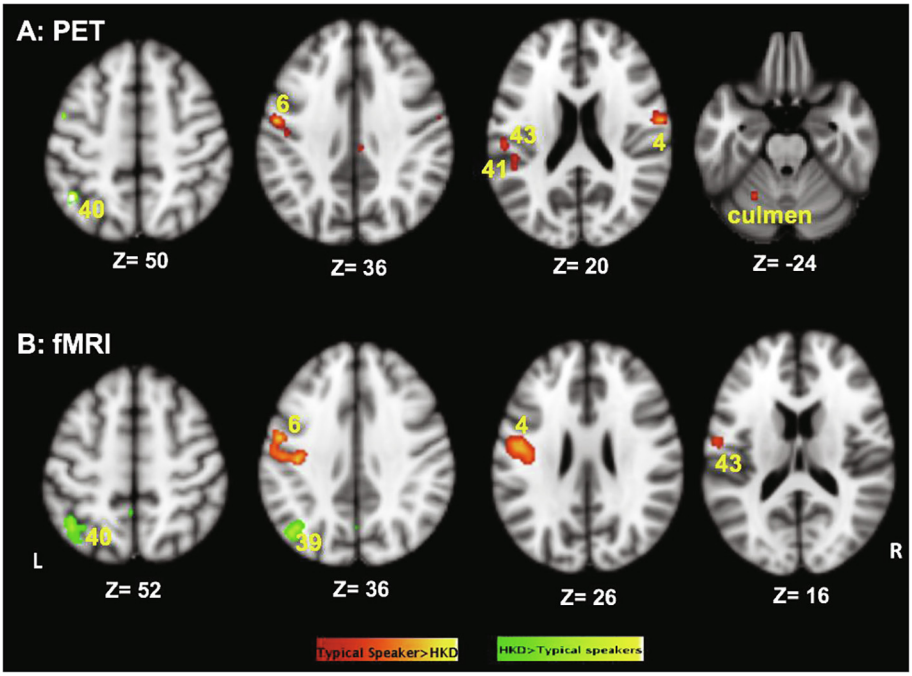

Fig. 7. Difference between the speech motor maps of typical speakers and speakers with HKD as derived by A. PET and B. fMRI. The left hemisphere is on the left side of the image. Activation maps in red denote typical speakers > Speakers with HKD and those in green denote Speakers with HKD > typical speakers contrasts. PET imaging found that when compared to typical speakers, speakers with HKD had decreased activity in left dorsal premotor (BA 6), opercular (BA 43), and auditory cortices (BA 41) and right M1 mouth/larynx (BA 4) and greater activity in left inferior parietal lobule (BA 40) during overt speaking. fMRI identified significant reductions in activity in left dorsal premotor (BA 6) and M1 mouth/larynx cortices (BA 4) and operculum (BA 43) and increased activity in left inferior parietal lobule (BA 40) and angular gyrus (BA 39) in speakers with HKD. (For interpretation of the references to colour in this figure legend, the reader is referred to the web version of this article.)

world speaking demands in both duration and content and more likely elicits the true extent of SPN deficits of HKD. Differences in brain areas found to be under- or over-active in HKD are likely due to the differences in tasks used as well as the nature and severity of HKD in the different cohorts. The differences between PET and fMRI results may also stem from differing mechanisms of cerebral blood flow changes (in PET) and the BOLD signal (in MRI). Additionally, artifacts from moving tongue, jaw and lips even when greatly reduced may still affect the resulting activation maps in fMRI.

Table 6
Differences in speech motor maps between typical speakers and speakers with HKD as identified by PET and fMRI.

Typical speakers > Speakers with HKD			PET				fMRI			
Lobe	Location	Brodmann area	x	y	z	Z score	x	y	z	Z score
Frontal	Precentral gyrus	6	−52	−8	34	7.7	−54	−4	38	3.3
	Medial frontal gyrus (SMA)	6	−12	−12	60	7.4				
	Precentral gyrus (M1 mouth)	4					−40	−16	34	3.4
	Precentral gyrus (M1 mouth)	4	60	−6	20	7.3				
Temporal	Superior temporal gyrus	41	−46	−34	18	6.0				
Parietal	Postcentral gyrus	43					−58	−8	16	2.7
	Postcentral gyrus	40	−54	−24	18	6.4				
Cerebellum	Culmen	Lobule VI	–22	−58	–22	6.2				
Speakers with HKD > Typical speakers										
Parietal	Inferior parietal lobule	40	−42	−56	48	6.0	−40	−58	52	5
	Angular gyrus	39					−46	−70	38	5.3

5. Potential drawbacks

One of the drawbacks of this study is that while PET and fMRI in typical speakers were performed on the same individuals, PET and fMRI data in HKD speakers were from different cohorts. Despite the two PD cohorts being similar in severity of PD (indexed by Hoehn and Yahr scores), the fMRI group had more participants, more older individuals, and better gender representation. The fMRI cohort had twice as many participants. Although majority of patients in both cohorts were between 50 and 70 years of age, the PET cohort included a 40 year-old individual and 40% of the fMRI cohort were between 70 and 80 years. Additionally, although the two groups were similar in their HKD symptoms and clinical evaluation, there could be differences in specific perceptual and acoustic indices of HKD. These factors might have contributed to the differences in activation patterns seen in PET and fMRI in the PD cohorts and the lower correlation coefficient noted between the speech motor networks in these cohorts. Future studies should attempt to enroll more participants with a more equal age and gender representation and include detailed perceptual and acoustic characterization of HKD. Another potential drawback in the comparisons between typical speakers and speakers with HKD is that the typical speakers were younger and not age-matched with the PD cohort. A recent study found that the rate and accuracy of performing diadochokinetic tasks deteriorated with age that related to decreased lip and tongue strength, decreased oral tactile sensitivity, and a decline in the neural planning and control of speech movements (Bilodeau-Mercure et al., 2015). A fMRI study of overt production of the vowels and trisyllabic utterances found that when compared to younger typical speakers (21–32 years), older typical speakers (62–84 years) relied less on the feedback system (indicated by decreased activity in the auditory processing regions) and depended more on the feedforward system (demonstrated by greater activation in bilateral SMA and inferior frontal gyri) (Sörös et al., 2011). Indeed, similar compensatory changes in the feedforward system has been observed in females with PD having mild hypophonia (Rektorova et al., 2007). However, in a pilot study with seven healthy elderly, right-handed females (mean age 63 ± 7.2 years) with no history of motor speech disorders who performed the same overt continuous speech paradigm in fMRI, we found no significant difference in the activation patterns between the younger typical speakers and the elderly typical speakers. Further, similar to a report in speakers with moderate HKD (Saxena et al., 2014), we found decreased activity in areas of SPN in the fMRI HKD cohort when compared to the elderly cohort (unpublished data). Therefore, we do not expect age-related changes to be a significant factor influencing the findings reported here.

6. Conclusions and future directions

The findings from this study demonstrate that SPN can be successfully obtained by fMRI using an overt continuous speech paradigm and that the maps strongly correlated with the speech motor maps identified by PET in a large cohort of typical speakers. Additionally, we used the new overt continuous reading paradigm to derive SPN in individuals with PD having HKD. We found that these data were reasonably comparable with the SPN identified in an earlier PET study using the reading paradigm in another cohort of individuals with HKD secondary to PD (Mefferd and Bissmeyer, 2016). Using both imaging modalities, we demonstrated that speakers with HKD have significantly decreased activity in critical feedforward (bilateral dorsal premotor and motor cortices) and feedback (auditory and somatosensory areas) subsystems mediating speech motor control. Therefore, we believe that SPNs can be reliably mapped using the new fMRI overt speech paradigm. Future studies should further examine the utility of this paradigm in investigating neural networks in other motor speech and voice disorders. Future studies should also examine whether this new fMRI speech paradigm is useful in examining the neural correlates of behavioral, surgical, and pharmacological interventions in motor speech disorders.

CRediT authorship contribution statement

Shalini Narayana: Conceptualization, Methodology, Investigation, Resources, Writing - original draft, Writing - review & editing, Supervision, Project administration, Funding acquisition. **Megan B. Parsons:** Formal analysis, Writing - original draft, Writing - review & editing, Visualization. **Wei Zhang:** Methodology, Formal analysis, Investigation, Data curation, Project administration, Writing - review & editing. **Crystal Franklin:** Formal analysis, Software, Resources, Writing - review & editing. **Katherine Schiller:** Methodology, Formal analysis, Investigation, Data curation, Project administration, Writing - review & editing. **Asim F. Choudhri:** Conceptualization, Investigation, Resources, Writing - review & editing. **Peter T. Fox:** Conceptualization, Methodology, Resources, Writing - review & editing, Supervision, Project administration, Funding acquisition. **Mark S. LeDoux:** Conceptualization, Investigation, Resources, Writing - review & editing. **Michael Cannito:** Conceptualization, Investigation, Resources, Writing - review & editing.

Acknowledgements

The authors thank Betty Heyl (PET technologist), Paul Jerabek, Ph.D. (Radiotracer preparation), Casey Strickland, BS (participant screening and data acquisition), Bella Bydlinski, MS (participant screening and data acquisition), and Caroline Royal-Evans, MS, CCP (speech and voice screening in individuals with Parkinson's disease).

Funding

This work was supported by the National Institutes of Health [grant numbers R21-DC009467 (SN), NS43738 (PTF)]; The Michael J. Fox Foundation for Parkinson Research, Therapeutic Pipeline award (SN); and The Le Bonheur Neuroscience Institute, Memphis TN.

References

Price, C.J., 2010. The anatomy of language: a review of 100 fMRI studies published in 2009. Ann. N. Y. Acad. Sci. 1191, 62–88.
Price, C.J., 2012. A review and synthesis of the first 20years of PET and fMRI studies of heard speech, spoken language and reading. NeuroImage. 62, 816–847.
Brown, S., Laird, A.R., Pfordresher, P.Q., Thelen, S.M., Turkeltaub, P., Liotti, M., 2009. The somatotopy of speech: Phonation and articulation in the human motor cortex. Brain Cogn. 70, 31–41.
Abo, M., Kasahara, K., Kakuda, W., Senoo, A., 2009. Functional MRI activation in repetition task using block and event-related design. J Appl Res. 9, 119–122.
Guenther, FH, 2016. Neural Control of Speech. The MIT Press, Cambridge MA, London England.
Hesling, I., Labache, L., Joliot, M., Tzourio-Mazoyer, N., 2019. Large-scale plurimodal networks common to listening to, producing and reading word lists: an fMRI study combining task-induced activation and intrinsic connectivity in 144 right-handers. Brain Struct. Funct. 224 (9), 3075–3094.
Tourville, J.A., Nieto-Castañón, A., Heyne, M., Guenther, F.H., 2019. Functional Parcellation of the Speech Production Cortex. J Speech Lang Hear Res. 62, 3055–3070.
Palmer, E.D., Rosen, H.J., Ojemann, J.G., Buckner, R.L., Kelley, W.M., Petersen, S.E., 2001. An Event-Related fMRI Study of Overt and Covert Word Stem Completion. NeuroImage. 14, 182–193.
Barch, D.M., Sabb, F.W., Carter, C.S., Braver, T.S., Noll, D.C., Cohen, J.D., 1999. Overt Verbal Responding during fMRI Scanning: Empirical Investigations of Problems and Potential Solutions. NeuroImage. 10, 642–657.
Huang, J., Carr, T.H., Cao, Y., 2002. Comparing cortical activations for silent and overt speech using event-related fMRI. Hum. Brain Mapp. 15, 39–53.
Shuster, L., Lemieux, S., 2005. An fMRI investigation of covertly and overtly produced mono- and multisyllabic words. Brain Lang. 93, 20–31.
Numminen, J., Curio, G., 1999. Differential effects of overt, covert and replayed speech on vowel-evoked responses of the human auditory cortex. Neurosci. Lett. 272, 29–32.
Ryding, E., BraÅdvik, B., Ingvar, D.H., 1996. Silent Speech Activates Prefrontal Cortical Regions Asymmetrically, as Well as Speech-Related Areas in the Dominant Hemisphere. Brain Lang. 52, 435–451.
Arnold, C., Gehrig, J., Gispert, S., Seifried, C., Kell, C.A., 2014. Pathomechanisms and compensatory efforts related to Parkinsonian speech. NeuroImage Clin. 4, 82–97.
Partovi, S., Konrad, F., Karimi, S., et al., 2012. Effects of Covert and Overt Paradigms in Clinical Language fMRI. Acad. Radiol. 19, 518–525.
Kielar, A., Milman, L., Bonakdarpour, B., Thompson, C.K., 2011. Neural correlates of covert and overt production of tense and agreement morphology: Evidence from fMRI. J. Neurolinguistics 24, 183–201.
Tourville, J.A., Reilly, K.J., Guenther, F.H., 2008. Neural mechanisms underlying auditory feedback control of speech. NeuroImage 39, 1429–1443.
Levelt, W.J., Roelofs, A., Meyer, A.S., 1999. A theory of lexical access in speech production. Behav Brain Sci. 22, 1–75.
Kemeny, S., Ye, F.Q., Birn, R., Braun, A.R., 2005. Comparison of continuous overt speech fMRI using BOLD and arterial spin labeling. Hum. Brain Mapp. 24, 173–183.
Troiani, V., Fernández-Seara, M.A., Wang, Z., Detre, J.A., Ash, S., Grossman, M., 2008. Narrative speech production: An fMRI study using continuous arterial spin labeling. NeuroImage. 40, 932–939.
Amaro, E., Barker, G.J., 2006. Study design in fMRI: Basic principles. Brain Cogn. 60, 220–232.
Birn, R.M., Bandettini, P.A., Cox, R.W., Jesmanowicz, A., Shaker, R., 1998. Magnetic field changes in the human brain due to swallowing or speaking. Magn. Reson. Med. 40, 55–60.
Birn, R.M., Bandettini, P.A., Cox, R.W., Shaker, R., 1999. Event-related fMRI of tasks involving brief motion. Hum. Brain Mapp. 7, 106–114.
J. Appl. Physiol. 83 (5), 1438–1447. https://doi.org/10.1152/jappl.1997.83.5.1438.
Baum, S.R., McFarland, D.H., Diab, M., 1996. Compensation to articulatory perturbation: Perceptual data. J Acoust Soc Am. Acoustical Society of. America 99, 3791–3794.
Lane, H., Denny, M., Guenther, F.H., et al., 2005. Effects of bite blocks and hearing status on vowel production. J. Acoust. Soc. Am. 118, 1636–1646.
Solomon, N.P., Makashay, M.J., Munson, B., 2016. The Effect of Jaw Position on Perceptual and Acoustic Characteristics of Speech. Int J Orofac Myol. 42, 15–24.
Tamura, T., Kanayama, T., Yoshida, S., Kawasaki, T., 2002. Analysis of brain activity during clenching by fMRI. J. Oral Rehabil. 29, 467–472.
Kelso, J.A.S., Tuller, B., 1983. "Compensatory Articulation" Under Conditions of Reduced Afferent Information: A Dynamic Formulation. J Speech Lang Hear Res. 26, 217–224.
Gay, T., Lindblom, B., Lubker, J., 1981. Production of bite-block vowels: Acoustic equivalence by selective compensation. J. Acoust. Soc. Am. 69, 802–810.
Lindblom, B., Lubker, J., Gay, T., 1977. Formant frequencies of some fixed-mandible vowels and a model of speech motor programming by predictive simulation. J. Acoust. Soc. Am. 62, S15.
McFarland, D.H., Baum, S.R., Chabot, C., 1996. Speech compensation to structural modifications of the oral cavity. J. Acoust. Soc. Am. 100, 1093–1104.
Smith, B.L., 1987. Effects of Bite Block Speech on Intrinsic Segment Duration. Phonetica. 44, 65–75.
Sussman, H.M., Fruchter, D., Cable, A., 1995. Locus equations derived from compensatory articulation. J. Acoust. Soc. Am. 97, 3112–3124.
Gabbert, G., 2005. Speech Production in Parkinson's Disease [Ph.D. Dissertation]. The University of Texas at Dallas.
Mefferd, A., Bissmeyer, M., 2016. Bite block effects on vowel acoustics in talkers with amyotrophic lateral Sclerosis and Parkinson's Disease. J. Acoust. Soc. Am. 140, 3442.
Duffy, J.R., 2005. Motor speech disorders: Substrates, differential diagnosis, and management, 2nd Edition. Mosby, St Louis, MO.
Ho, A.K., Iansek, R., Marigliani, C., Bradshaw, J.L., Gates, S., 1999. Speech impairment in a large sample of patients with Parkinson's disease. Behav. Neurol. 11, 131–137.
Narayana, S., Fox, P.T., Zhang, W., et al., 2010. Neural correlates of efficacy of voice therapy in Parkinson's disease identified by performance-correlation analysis. Hum. Brain Mapp. 31, 222–236.
Pinto, S., Thobois, S., Costes, N., et al., 2004. Subthalamic nucleus stimulation and dysarthria in Parkinson's disease: a PET study. Brain. 127, 602–615.
Rektorova, I., Barrett, J., Mikl, M., Rektor, I., Paus, T., 2007. Functional abnormalities in the primary orofacial sensorimotor cortex during speech in Parkinson's disease. Mov. Disord. 22, 2043–2051.
Saxena, M., Behari, M., Kumaran, S.S., Goyal, V., Narang, V., 2014. Assessing speech dysfunction using BOLD and acoustic analysis in parkinsonism. Parkinsonism Relat Disord. 20, 855–861.
Maillet, A., Krainik, A., Debû, B., et al., 2012. Levodopa Effects on Hand and Speech Movements in Patients with Parkinson's Disease: A fMRI Study. Meck WH, editor. PLoS ONE 7, e46541.
Pinto, S., Mancini, L., Jahanshahi, M., et al., 2011. Functional magnetic resonance imaging exploration of combined hand and speech movements in Parkinson's disease. Mov. Disord. 26, 2212–2219.
Liotti, M., Ramig, L.O., Vogel, D., et al., 2003. Hypophonia in Parkinson's disease: neural correlates of voice treatment revealed by PET. Neurology. 60, 432–440.
Oldfield, R.C., 1971. The assessment and analysis of handedness: the Edinburgh inventory. Neuropsychologia. 9, 97–113.
Darley, F., Aronson, A., Brown, J., 1975. Motor Speech Disorders. W.B. Saunders Inc., Philadelphia, PA.
Fox, P.T., Narayana, S., Tandon, N., et al., 2006. Intensity modulation of TMS-induced cortical excitation: Primary motor cortex. Hum. Brain Mapp. 27, 478–487.
Fox, P.T., Ingham, R.J., Ingham, J.C., Zamarripa, F., Xiong, J.H., Lancaster, J.L., 2000. Brain correlates of stuttering and syllable production. A PET performance-correlation analysis. Brain. J. Neurol. 123 (Pt 10), 1985–2004.
Fox, P.T., Raichle, M.E., 1984. Stimulus rate dependence of regional cerebral blood flow in human striate cortex, demonstrated by positron emission tomography. J. Neurophysiol. 51, 1109–1120.
Van Riper, C., 1963. Speech correction: principles and methods, 4th Edition. Prentice Hall, Englewood Cliffs, NJ.
Fairbanks, G., 1960. Voice and articulation drillbook. Harper and Row, New York, NY.
Smith, S.M., 2002. Fast robust automated brain extraction. Hum. Brain Mapp. 17, 143–155.
Smith, S.M., Jenkinson, M., Woolrich, M.W., et al., 2004. Advances in functional and structural MR image analysis and implementation as FSL. NeuroImage. 23, S208–S219.
Jenkinson, M., Bannister, P., Brady, M., Smith, S., 2002. Improved Optimization for the Robust and Accurate Linear Registration and Motion Correction of Brain Images. NeuroImage. 17, 825–841.
Fox, P.T., Mintun, M.A., Reiman, E.M., Raichle, M.E., 1988. Enhanced Detection of Focal Brain Responses Using Intersubject Averaging and Change-Distribution Analysis of Subtracted PET Images. J. Cereb. Blood Flow Metab. 8, 642–653.
Fox, P.T., Mintun, M.A., 1989. Noninvasive Functional Brain Mapping by Change-Distribution Analysis of Averaged PET Images of H2150 Tissue Activity. J. Nucl. Med. 30, 141–149.
Mintun, M.A., Fox, P.T., Raichle, M.E., 1989. A Highly Accurate Method of Localizing Regions of Neuronal Activation in the Human Brain with Positron Emission Tomography. J. Cereb. Blood Flow Metab. 9, 96–103.
Worsley, K.J., 2001. Statistical analysis of activation images. Funct MRI Introd Methods. Oxford University Press, Oxford, pp. 251–270.
Beckmann, C.F., Jenkinson, M., Smith, S.M., 2003. General multilevel linear modeling for group analysis in FMRI. NeuroImage. 20, 1052–1063.
Woolrich, M.W., Behrens, T.E.J., Beckmann, C.F., Jenkinson, M., Smith, S.M., 2004. Multilevel linear modelling for FMRI group analysis using Bayesian inference. NeuroImage. 21, 1732–1747.
Woolrich, M., 2008. Robust group analysis using outlier inference. NeuroImage 41, 286–301.
Smith, S.M., Fox, P.T., Miller, K.L., et al., 2009. Correspondence of the brain's functional architecture during activation and rest. Proc. Natl. Acad. Sci. 106, 13040–13045.
Penfield, W., Rasmussen, T., 1950. The cerebral cortex of man; a clinical study of localization of function. Macmillan, New York, NY.
Grabski, K., Lamalle, L., Vilain, C., et al., 2012. Functional MRI assessment of orofacial articulators: Neural correlates of lip, jaw, larynx, and tongue movements. Hum. Brain Mapp. 33, 2306–2321.
Turkeltaub, P.E., Eden, G.F., Jones, K.M., Zeffiro, T.A., 2002. Meta-Analysis of the Functional Neuroanatomy of Single-Word Reading: Method and Validation. NeuroImage 16, 765–780.
Brown, S., Ingham, R.J., Ingham, J.C., Laird, A.R., Fox, P.T., 2005. Stuttered and fluent speech production: An ALE meta-analysis of functional neuroimaging studies. Hum. Brain Mapp. 25, 105–117.
Seghier, M.L., Hope, T.M.H., Prejawa, S., Jonesiwi, Parker, Vitkovitch, M., Price, C.J.,

2015. A Trade-Off between Somatosensory and Auditory Related Brain Activity during Object Naming But Not Reading. J. Neurosci. 35, 4751–4759.
Yamamoto, A.K., Parker Jones, O., Hope, T.M.H., et al., 2019. A special role for the right posterior superior temporal sulcus during speech production. NeuroImage 203, 116184.
Mahler, L.A., Ramig, L.O., Fox, C., 2015. Evidence-based treatment of voice and speech disorders in Parkinson disease. Curr. Opin. Otolaryngol. Head Neck Surg. 23, 209–215.
Smith, M.E., Ramig, L.O., Dromey, C., Perez, K.S., Samandari, R., 1995. Intensive voice treatment in parkinson disease: Laryngostroboscopic findings. J. Voice 9, 453–459.
Cannito, M.P., Suiter, D.M., Beverly, D., Chorna, L., Wolf, T., Pfeiffer, R.M., 2012. Sentence Intelligibility Before and After Voice Treatment in Speakers With Idiopathic Parkinson's Disease. J. Voice 26, 214–219.
Brabenec, L., Klobusiakova, P., Barton, M., et al., 2019. Non-invasive stimulation of the auditory feedback area for improved articulation in Parkinson's disease. Parkinsonism Relat Disord 61, 187–192.
Sachin, S., Senthil Kumaran, S., Singh, S., et al., 2008. Functional mapping in PD and PSP for sustained phonation and phoneme tasks. J. Neurol. Sci. 273, 51–56.
Riecker, A., Kassubek, J., Gröschel, K., Grodd, W., Ackermann, H., 2006. The cerebral control of speech tempo: Opposite relationship between speaking rate and BOLD signal changes at striatal and cerebellar structures. NeuroImage. 29, 46–53.
Péran, P., Nemmi, F., Méligne, D., et al., 2013. Effect of levodopa on both verbal and motor representations of action in Parkinson's disease: A fMRI study. Brain Lang. 125, 324–329.
Rektorova, I., Mikl, M., Barrett, J., Marecek, R., Rektor, I., Paus, T., 2012. Functional neuroanatomy of vocalization in patients with Parkinson's disease. J. Neurol. Sci. 313, 7–12.
Bilodeau-Mercure, M., Kirouac, V., Langlois, N., Ouellet, C., Gasse, I., Tremblay, P., 2015. Movement sequencing in normal aging: speech, oro-facial, and finger movements. AGE. 37, 78.
Sörös, P., Bose, A., Sokoloff, L.G., Graham, S.J., Stuss, D.T., 2011. Age-related changes in the functional neuroanatomy of overt speech production. Neurobiol. Aging 32, 1505–1513.
Woolrich, M.W., Ripley, B.D., Brady, M., Smith, S.M., 2001. Temporal Autocorrelation in Univariate Linear Modeling of FMRI Data. NeuroImage 14 (6), 1370–1386. https://doi.org/10.1006/nimg.2001.0931.